ChemComm

COMMUNICATION

View Article Online
View Journal | View Issue

Cite this: *Chem. Commun.*, 2021, **57**, 3006

Received 6th July 2020,
Accepted 1st February 2021

DOI: 10.1039/d0cc04670a

rsc.li/chemcomm

The discovery of SKLB-0335 as a paralog-selective EZH2 covalent inhibitor†

Qiangsheng Zhang,‡[a] Xi Hu,‡[a] Lu Li,‡[b] Lidan Zhang,[a] Guoquan Wan,[a] Qiang Feng,[c] Yongxia Zhu,[d] Ningyu Wang,*[e] Zhihao Liu*[a] and Luoting Yu *[a]

By targeting the unique Cys663 of EZH2, SKLB-0335 displays high paralog-selectivity on EZH2. Biochemical studies show that SKLB-0335 can covalently bind to EZH2 at its S-adenosylmethionine (SAM) pocket and inhibit H3K27Me3. SKLB-0335 could be an effective chemical probe with which to further investigate the specific biological functions of EZH2.

Polycomb repressive complex 2 (PRC2) is composed of one catalytic subunit, enhancer of zeste homologue (EZH) 1 or EZH2, two core members, suppressor of zeste 12 (SUZ12) and embryonic ectoderm development (EED) and additional subunits.[1] PRC2 catalyzes the trimethylation of the Lys 27 of histone H3 (H3K27Me3), which is an epigenetic mark of transcriptionally repressed and silenced target genes. Dysregulation of the PRC2 function correlates with certain malignancies and poor prognosis. The mutation, amplification, and/or overexpression of EZH2 has been implicated in numerous blood and solid tumors.[2]

EZH2 and EZH1 are highly homologous, sharing 76% overall sequence identity and 96% sequence identity in their catalytic su(var)3-9, enhancer-of-zeste and trithorax (SET) domains.[3] In specific tumors, the inhibition of EZH2 alone exerts significant anti-proliferative activity, which means that the inhibition of both EZH2 and EZH1 is unnecessary, such as in diffuse large B-cell lymphomas.[4] The functions of EZH2 and EZH1 mainly differ in two ways: (1) EZH2 and EZH1 are expressed in opposite ways during development and cell differentiation. EZH2 is dominant in proliferating cells, while EZH1 is dominant in postmitotic tissues;[5] (2) PRC2 that contains EZH1 directly and robustly represses transcription from chromatinized templates and compacts chromatin, while PRC2 that contains EZH2 does not.[6] EZH performs some other biological functions in a PRC2-independent manner. EZH2 trimethylates not only H3K27, but also nonhistone proteins such as STAT3 and RORα.[7,8] EZH1 also plays an important role in differentiation, regeneration and immunity.[9–11]

The development of EZH2 inhibitors has been intensely studied. Several EZH2 inhibitors have demonstrated promising antitumor activity in preclinical and clinical trials, such as EPZ-6438 (Tazemetostat), CPI-1205, GSK126, ZLD1039, (R)-OR-S1 and GNA002.[12–14] GNA002, a derivative of gambogenic acid, is the first reported covalent inhibitor of EZH2. However, most of these inhibitors are less selective for EZH1/EZH2 (Fig. 1). As such, they are not effective chemical probes with which to study the specific biological functions of EZH2. The distinct functions of EZH1 and EZH2 suggest that selectively targeting EZH2 may result in a different efficacy and tolerability profile compared with dual-EZH1/EZH2 inhibitors. To enable the specific functions of EZH2 to be investigated, we have developed and characterized potent, highly paralog-selective EZH2 inhibitors.

We identified a unique cysteine 663 (Cys663) residue in the SET region of EZH2 as an effective target for selective inhibition after aligning the sequences of EZH2 and EZH1 (Fig. 2A and B).[15] A search of the International Cancer Genome Consortium (ICGC) database also revealed that no Cys663 mutation in EZH2 has yet been reported (Fig. S1, ESI†). Therefore, we hypothesized that targeting Cys663 as a covalent coupling site might achieve a higher selectivity for EZH2 than EZH1.

By analyzing the co-crystal structures of multiple compounds complexed with PRC2, we found that indole derivatives were the

[a] *State Key Laboratory of Biotherapy/Collaborative Innovation Center for Biotherapy, West China Hospital, West China Medical School, Sichuan University, Chengdu, Sichuan 610041, P. R. China. E-mail: liuzhihao@scu.edu.cn, yuluot@scu.edu.cn*
[b] *Institute of Clinical Trials, West China Hospital, Sichuan University, Chengdu, Sichuan, 610041, P. R. China*
[c] *College of Chemistry and Life Science, Chengdu Normal University, Chengdu 611130, P. R. China*
[d] *Department of Clinical Pharmacy, Sichuan Cancer Hospital & Institute, Sichuan Cancer Center, School of Medicine, University of Electronic Science and Technology of China, Chengdu, 610041, P. R. China*
[e] *School of Life Science and Engineering, Southwest JiaoTong University, Chengdu, Sichuan, 611756, P. R. China. E-mail: wangny-swjtu@swjtu.edu.cn*

† Electronic supplementary information (ESI) available: Experimental procedures, characterization data, and additional spectra. See DOI: 10.1039/d0cc04670a

‡ These authors contributed equally to this work.

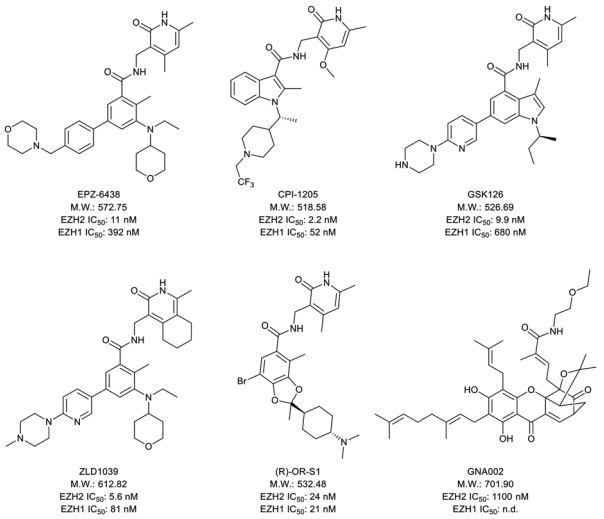

Fig. 1 Representative EZH2 inhibitors (n.d. = not determined).

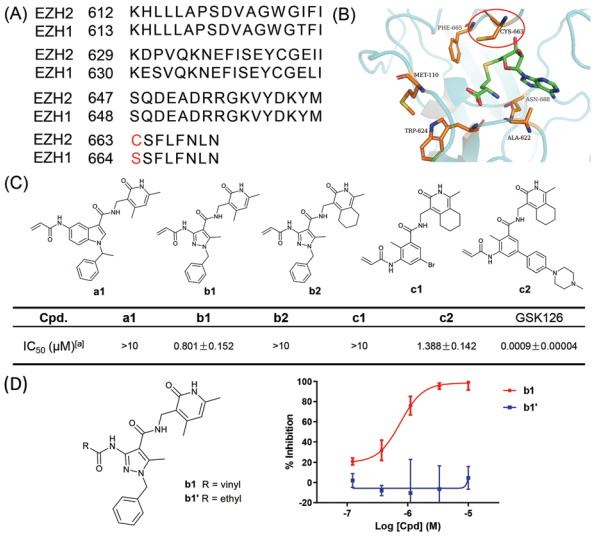

Fig. 2 (A) The sequence alignment of the SET domains of EZH2 and EZH1. (B) Cys663 is in the vicinity of the ligand-binding site (PDB code: 5HYN); carbons are shown in green for *S*-adenosylhomocysteine. (C) The chemical structures of the first five compounds and their IC_{50} values on $EZH2^{WT}$. [a]Data are expressed as mean ± SEM from at least two independent experiments. (D) Inhibition curves of compound **b1** and its reversible analog **b1′** on $EZH2^{WT}$. Data are expressed as mean ± SD (n = 2).

most suitable for introducing electrophilic warheads (Fig. S2, ESI†). An acrylamide group, which is easy to synthesize and is inert to glutathione (GSH),[16] was introduced at the 5 position of the indole ring to form a covalent bond with Cys663. We also reduced the indole ring to pyrazole and benzene rings, given that the increased flexibility of the molecule makes it easier to form a covalent bond through Michael addition (Fig. S3, ESI†). The target compounds were synthesized *via* a four–six step procedure from commercially available 5-nitro-1*H*-indole-3-carboxylic acid (Scheme S1, ESI†), 5-amino-3-methyl-1*H*-pyrazole-4-carboxylate (Scheme S2, ESI†) and methyl 5-bromo-2-methyl-3-nitrobenzoate (Scheme S3, ESI†).

Of the first five compounds generated, compounds **b1** and **c2** inhibited the activity of EZH2 at the micromolar level (Fig. 2C). To preliminarily verify whether these two compounds exert an inhibitory effect by covalently binding to EZH2, their reversible analogs, compounds **b1′** and **c2′**, were synthesized (Fig. S4, ESI†). Compared to compound **b1**, the inhibitory activity of compound **b1′** on $EZH2^{WT}$ is significantly reduced (Fig. 2D). The activities of compounds **c2′** and **c2** are comparable. However, we could not determine whether this type of compound binds covalently to EZH2 (Fig. S5, ESI†). We therefore focused on pyrazole derivatives in the following work.

To obtain more potent inhibitors, we studied the structure–activity relationships of pyrazole derivatives (Table S1, ESI†). It was found that the activity was significantly reduced if the pyridone ring C4–C5 positions together formed a cyclohexane or two ethyl groups were introduced at the C4 and C6 positions. When a larger group, such as a biphenyl group, was introduced at the R^2 position, compounds **b12–b15** were slightly less active than when a benzene substituent was present. Compounds **b4**, **b6** and **b7** with a methyl substitution at the R^1 position were found to be more potent than the unsubstituted compounds **b8**, **b10** and **b11**. If a methyl group was introduced on the methylene at the benzyl substituted at the R^2 position, compound **b4** was 12-fold more active than compound **b1**. Notably, compound **(R)-b4** exhibited the most potent activity among the synthesized compounds. Compound **b4** (SKLB-0335) was therefore selected for further research because it has comparable activity to that of **(R)-b4** and is easier to synthesize.

The reversible analog of SKLB-0335 was synthesized as a control (Fig. 3A). Compared to SKLB-0335, the inhibitory activity of SKLB-0335′ on $EZH2^{WT}$ was significantly reduced. For incubation times of 15 to 120 min, the inhibitory activity of SKLB-0335 was improved, while the activities of GSK126 and SKLB-0335′ were not (Fig. 3B). Molecular modeling studies show that SKLB-0335 binds to the SAM pocket of EZH2 (Fig. 3C). SKLB-0335 displays an extremely slow off-rate (k_{off}) of 0.00347 min^{-1}, which results in a residence time half-life ($t_{1/2}$) of 199.8 min (Fig. 3D). To further demonstrate that SKLB-0335 binds to the SAM pocket of PRC2 and exerts its inhibitory activity by forming a covalent bond, we performed competitive experiments using different concentrations of SAM. When the incubation time was 15 min, the inhibitory activities of SKLB-0335 and GSK126 decreased by around 10-fold as the SAM concentration increased from 3 to 30 μM. When the incubation time was extended to 120 min, the inhibitory activity of GSK126 still decreased with an increase in SAM. However, the inhibitory activity of SKLB-0335 showed no significant changes. Over time, SKLB-0335 bound covalently to EZH2 and its activity was no longer affected by the concentration of its substrate, SAM (Fig. 3E). To confirm that SKLB-0335 specifically reacts with cysteine, SKLB-0335 was incubated with purified EZH2 containing the full SET domain and then analyzed using mass spectrometry (MS). The MS analyses reveal that a peak at +433.75 Da could be observed for the probe-EZH2 adduct from the unmodified EZH2, with no detectable unmodified EZH2, indicating that SKLB-0335 efficiently forms a single modified covalent adduct (Fig. 3F). We also tested the

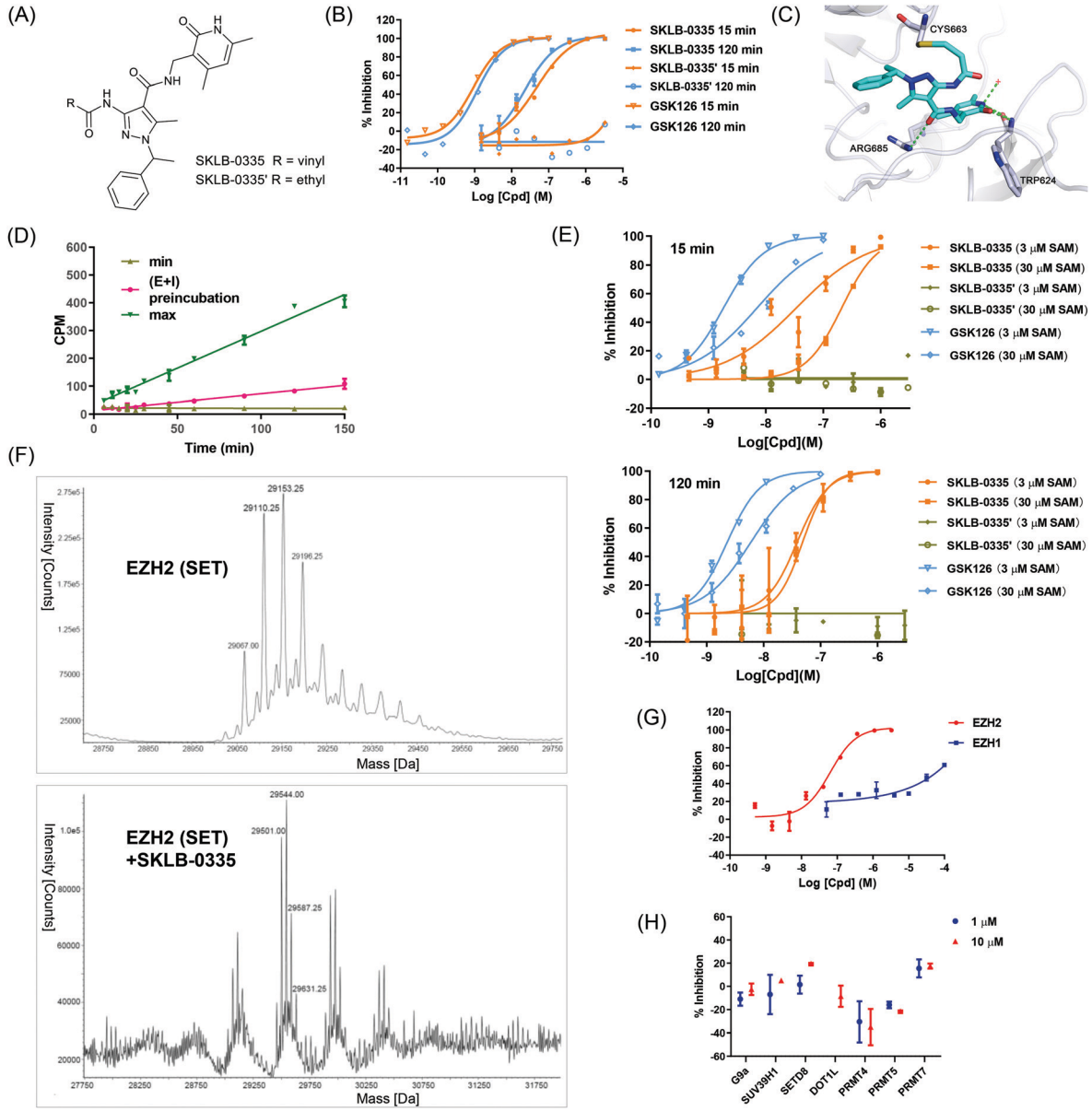

Fig. 3 (A) Chemical structures of SKLB-0335 and SKLB-0335′. (B) The inhibition curves of EZH2^{WT} for SKLB-0335, SKLB-0335′, and GSK126 with 15 and 120 min of incubation. (C) The predicted binding mode of SKLB-0335 (PDB code: 5LS6). Green dashed lines: hydrogen bonds. (D) The k_{off} progress curve on SKLB-0335 against EZH2 (E = enzyme, I = inhibitor). (E) The SAM competitive inhibition of SKLB-0335, SKLB-0335′, and GSK126 with 15 and 120 min of incubation. (F) Mass spectra of EZH2 alone and EZH2 preincubated with SKLB-0335 (MW:433.51). (G) The inhibition curves for EZH2 and EZH1 of SKLB-0335. (H) The SKLB-0335 inhibition of G9a, SUV39H1, SETD8, DOT1L, PRMT4, PRMT5, and PRMT7. Data are expressed as mean ± SD (n = 2).

paralog-selectivity of SKLB-0335 for EZH1/EZH2. The results show that the inhibitory activity of SKLB-0335 on EZH1 is 1500 times lower than that of EZH2 (Fig. 3G). They also show potent and concentration dependent inhibition of mutant EZH2, including EZH2^{Y641F}, EZH2^{Y641N} and EZH2^{A677G} (Fig. S6, ESI†). SKLB-0335 does not exhibit significant inhibition of the seven other tested methyltransferases (Fig. 3H).

The ability of SKLB-0335 to reduce H3K27Me3 was evaluated in SU-DHL-6 cells by western blot analysis. Treatment with SKLB-0335 potently abolished the H3K27Me3 marker in a time-dependent (Fig. 4A) and concentration-dependent manner (Fig. 4B). Furthermore, we treated the cells with SKLB-0335, SKLB-0335′ and GSK126 for six days, then fully washed them with compound-free medium, and assessed the changes in the H3K27Me3 levels over a period of 96 h. Recovery of H3K27Me3 in cells treated with SKLB-0335 was significantly slower than that those treated with GSK126 (Fig. 4C). We next analyzed the mRNA levels of CDX2, CCND2, BMP6 and EOMES, which are regulated by EZH1. All of these examined genes were significantly upregulated after GSK126 treatment. However, treatment with SKLB-0335 did not affect the mRNA expression of these genes both in SU-DHL-6 cells (Fig. 4D) and WSU-DLCL-2 cells (Fig. S7, ESI†). The results showed that SKLB-0335 could selectively inhibit EZH2 without affecting the biological function of EZH1.

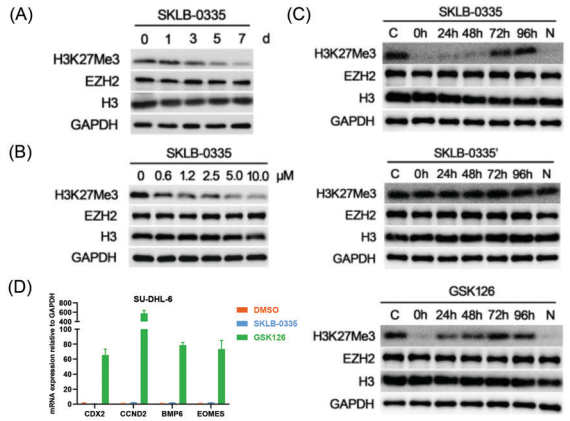

Fig. 4 (A) Time course of H3K27Me3 inhibition by SKLB-0335. (B) Dose-dependent inhibition of H3K27 methylation in SU-DHL-6 cells after 6 days of SKLB-0335 treatment. (C) Time course of H3K27Me3 inhibition after SKLB-0335, SKLB-0335′, and GSK126 were washed out of SU-DHL-6 cells (*N* = not washed out). Results are expressed as mean ± SD from at least three independent experiments. (D) RT-qPCR analysis of the mRNA levels of EZH1-related genes in SU-DHL-6 cells following treatment with compounds (10 μM for 5 days). Results are expressed as mean ± SD from at least three independent experiments.

In this study, a series of novel EZH2 covalent inhibitors was designed and synthesized. SKLB-0335 was found to be a potent and paralog-selective inhibitor of EZH2. This selectivity effectively circumvents concerns about toxicity due to the inhibition of EZH1 and other methyltransferases. From our findings, we proposed that SKLB-0335 covalently binds to the SAM pocket of EZH2. The findings that support this conclusion include MS results, kinetic studies, and some other biochemical assays. In summary, SKLB-0335 represents a potent, paralog-selective, covalent EZH2 inhibitor that could be an effective therapy for diseases driven by EZH2. SKLB-0335 could also be used as a chemical probe to further investigate the specific roles of EZH2, not EZH1/EZH2, in cancer and other related diseases.

This work was supported by the National Natural Science Foundation of China (81702946, 82073687) and the National S&T Major Special Project on Major New Drug Innovations of China (2018ZX09201018).

Conflicts of interest

There are no conflicts to declare.

Notes and references

1 A. Kuzmichev, K. Nishioka, H. Erdjument-Bromage, P. Tempst and D. Reinberg, *Genes Dev.*, 2002, **16**, 2893–2905.
2 H. P. Mohammad, O. Barbash and C. L. Creasy, *Nat. Med.*, 2019, **25**, 403–418.
3 X. Yang, F. Li, K. D. Konze, J. Meslamani, A. Ma, P. J. Brown, M. M. Zhou, C. H. Arrowsmith, H. U. Kaniskan, M. Vedadi and J. Jin, *J. Med. Chem.*, 2016, **59**, 7617–7633.
4 S. K. Knutson, T. J. Wigle, N. M. Warholic, C. J. Sneeringer, C. J. Allain, C. R. Klaus, J. D. Sacks, A. Raimondi, C. R. Majer, J. Song, M. P. Scott, L. Jin, J. J. Smith, E. J. Olhava, R. Chesworth, M. P. Moyer, V. M. Richon, R. A. Copeland, H. Keilhack, R. M. Pollock and K. W. Kuntz, *Nat. Chem. Biol.*, 2012, **8**, 890–896.
5 E. Ezhkova, W. H. Lien, N. Stokes, H. A. Pasolli, J. M. Silva and E. Fuchs, *Genes Dev.*, 2011, **25**, 485–498.
6 X. Shen, Y. Liu, Y. J. Hsu, Y. Fujiwara, J. Kim, X. Mao, G. C. Yuan and S. H. Orkin, *Mol. Cell*, 2008, **32**, 491–502.
7 G. Cavalli, *Science*, 2012, **338**, 1430–1431.
8 E. Kim, M. Kim, D.-H. Woo, Y. Shin, J. Shin, N. Chang, Y. T. Oh, H. Kim, J. Rheey and I. Nakano, *Cancer Cell*, 2013, **23**, 839–852.
9 L. T. Vo, M. A. Kinney, X. Liu, Y. Zhang, J. Barragan, P. M. Sousa, D. K. Jha, A. Han, M. Cesana and Z. Shao, *Nature*, 2018, **553**, 506–510.
10 S. Ai, X. Yu, Y. Li, Y. Peng, C. Li, Y. Yue, G. Tao, C. Li, W. T. Pu and A. He, *Circ. Res.*, 2017, **121**, 106–112.
11 Y. Liu, Q. Zhang, Y. Ding, X. Li, D. Zhao, K. Zhao, Z. Guo and X. Cao, *J. Immunol.*, 2015, **194**, 2838–2846.
12 R. Fioravanti, G. Stazi, C. Zwergel, S. Valente and A. Mai, *Chem. Rec.*, 2018, **18**, 1818–1832.
13 X. J. Song, T. T. Gao, N. Y. Wang, Q. Feng, X. Y. You, T. H. Ye, Q. Lei, Y. X. Zhu, M. H. Xiong, Y. Xia, F. F. Yang, Y. J. Shi, Y. Q. Wei, L. D. Zhang and L. T. Yu, *Sci. Rep.*, 2016, 6.
14 X. Wang, W. Cao, J. J. Zhang, M. Yan, Q. Xu, X. B. Wu, L. X. Wan, Z. Y. Zhang, C. P. Zhang, X. Qin, M. Xiao, D. X. Ye, Y. Y. Liu, Z. G. Han, S. M. Wang, L. Mao, W. Y. Wei and W. T. Chen, *EMBO J.*, 2017, **36**, 1243–1260.
15 N. Justin, Y. Zhang, C. Tarricone, S. R. Martin, S. Chen, E. Underwood, V. De Marco, L. F. Haire, P. A. Walker, D. Reinberg, J. R. Wilson and S. J. Gamblin, *Nat. Commun.*, 2016, **7**, 11316.
16 D. G. Hoch, D. Abegg and A. Adibekian, *Chem. Commun.*, 2018, **54**, 4501–4512.